

K. SZYSZKIEWICZ*, P. DZIEMBAJ*, R. FILIPEK*

HEAT TRANSFER AND INVERSE PROBLEMS; SELECTED CASES IN 1D AND 3D GEOMETRIES

TRANSPORT CIEPŁA I ZAGADNIENIA ODWROTNE; WYBRANE PRZYKŁADY W GEOMETRII JEDNO- I TRÓJWYMIAROWEJ

Heat transport phenomena in the framework of continuum media mechanics is presented. Equations for conservation laws and finite volume numerical method based on these equations are discussed. This method is the foundation of the FLUENT computational fluid dynamics (CFD) package which was used for calculations of the temperature distribution in several examples: steady and evolutionary states for single and multiphase systems. Comparison with analytical solutions was carried out. This allows verification of the FLUENT results for various boundary conditions. Independent procedure based on the method of lines was applied for 1D cases and compared with FLUENT and/or analytical results. Formulation of a special type inverse problem for heat equation was given. Analytical solution of the steady-state inverse problem in 1D geometry was developed. Analogous case for 3D geometry was tested using FLUENT. This led to the optimization problem with clear and well defined optimum. This result suggests that in similar but more general inverse problems global optimum may exist which justifies the inverse problem methodology.

Zaprezentowano zjawiska transportu ciepła w kontekście mechaniki ośrodków ciągłych. Omówiono równania wyrażające prawa zachowania oraz metodę numeryczną objętości skończonych bazującą na tych prawach. Metoda ta będąca podstawą pakietu FLUENT, który służy do obliczeń w dynamice płynów (CFD, computational fluid dynamics) została użyta do symulacji rozkładu temperatury w kilku przykładach ilustrujących stany ewolucyjne i stacjonarne dla jedno- i wielo-fazowych układów. Przeprowadzono porównanie z wybranymi rozwiązaniami analitycznymi. Pozwoliło to na weryfikację wyników z FLUENT-a dla różnych warunków brzegowych. Niezależna procedura oparta o metodę linii dla przypadku jednowymiarowego została wykorzystana do porównania z wynikami z FLUENT-a oraz wynikami analitycznymi. Sformułowano pewien specjalny przypadek zagadnienia odwrotnego dla równania ciepła i przedstawiono jego analityczne rozwiązanie. Analogiczny przypadek w geometrii trójwymiarowej przetestowano numerycznie z użyciem FLUENT-a. Prowadzi to do problemu optymalizacji z dobrze określonym minimum globalnym. Wynik ten sugeruje, że w podobnych, ale bardziej ogólnych zagadnieniach odwrotnych może istnieć optimum, co usprawiedliwia metodologię zagadnienia odwrotnego w takich sytuacjach.

1. Introduction

Today, the design of innovative, multifunction materials guaranteeing their optimal use in engineering applications, is impossible without computer modeling [6]. The impressive development of computational power of modern computers have made it possible to carry out huge and time-consuming scientific computations on standard PCs by virtually any user.

Material science is one of the most active areas of current research in computational heat transfer [1], [2], [3], [4]. For example, heat transfer and fluid flow are important in materials processing methods such as casting, chemical deposition, spray coating, welding, and blast furnace design and durability. Thus it is vital to understand these phenomena and develop procedures to control such effects. As a consequence of importance of heat and mass transfer and fluid flow, extensive work has been done directed at numerical modeling. An obvious advantage of computer modeling is that the behavior and

properties of a system may be analyzed without actually creating a prototype. Thus the total cost of product development can be significantly reduced.

The basic equations describing fluid flow and heat transfer were already known at the beginning of XIX century [5]. However, the numerical methods to solve them for real-world engineering applications became feasible in the second half of the XX century due to the appearance of computers.

The main goal of the paper is to present wide-range simulations and possible use of inverse problems involving heat transfer phenomena by using specialized commercial CFD software (FLUENT) and authors' own programs for comparing results. Also we advocate the use of special cases where analytical solutions can be obtained for testing purposes.

The most popular numerical method used in the CFD is the finite volume method. It requires the equations to be written in the form of conservation laws so we start with short introduction to the basic models of CFD.

* FACULTY OF MATERIALS SCIENCE AND CERAMICS, AGH UNIVERSITY OF SCIENCE AND TECHNOLOGY, 30-059 KRAKÓW, 30 MICKIEWICZA AV., POLAND

2. Conservation laws for continuum media

The governing equations of heat and mass transport represent mathematical statements of the conservation laws of physics. Basically in all situations we can resort to the following conservation laws: the mass conservation law, the rate of change of momentum law (equal to the sum of all forces on the fluid element (Newton's second law)), the rate of change of energy law (equal to the rate of heat input and the rate of work done on the fluid element – the energy conservation law or the first law of thermodynamics) [6], [7].

We consider a system of r species (components) occupying a region Ω in space \mathbb{R}^3 with $\rho_i(x, t)$ being the mass density of the i -th species. We assume that all species move according to a velocity vector field $\mathbf{v}(x, t)$ in Ω which describes the velocity at position $x \in \mathbb{R}^3$ and time instant $t \geq 0$.

Mass conservation of i -th species can be stated in words as

$$\left[\begin{array}{c} \text{rate of change} \\ \text{of mass in an element} \end{array} \right] = \left[\begin{array}{c} \text{net rate of flow} \\ \text{of mass into an element} \end{array} \right] + \left[\begin{array}{c} \text{rate of production/consumption} \\ \text{of mass in an element} \end{array} \right]$$

and the formal expression for this law is

$$\frac{\partial \rho_i}{\partial t} + \text{div}(\rho_i \mathbf{v} + \mathbf{J}_i^d) = R_i \quad (i = 1, \dots, r), \quad (1)$$

where: \mathbf{J}_i^d – the diffusion flux of i th species ($\text{kg} \cdot \text{m}^{-2} \cdot \text{s}^{-1}$), R_i – the rate of production/destruction of i th species per unit volume. From eq. (1) we see that the movement of mass is split into two terms: convective ($\rho_i \mathbf{v}$), caused by the general flow and diffusion transport (\mathbf{J}_i^d), normally caused by the gradient of mass distribution.

If the diffusion flux \mathbf{J}_i^d is expressed by the use of Fick's law of diffusion, $\mathbf{J}_i^d = -\theta_i \nabla \rho_i$, where θ_i is the diffusion coefficient, then eq. (1) can be written as

$$\frac{\partial \rho_i}{\partial t} + \text{div}(\rho_i \mathbf{v}) = \text{div}(\theta_i \nabla \rho_i) + R_i \quad (i = 1, \dots, r). \quad (2)$$

Momentum equation

This fundamental equation is based on the Newton's second law – a cornerstone of classical mechanics. In words it states that

$$\left[\begin{array}{c} \text{rate of change of} \\ \text{momentum of an element} \end{array} \right] = \left[\begin{array}{c} \text{sum of all forces acting} \\ \text{on the element} \end{array} \right]$$

The rates of change of momentum components (per unit volume) is given by $\rho \frac{Dv_\alpha}{Dt}$, where $\alpha \in \{x, y, z\}$ and $\frac{D}{Dt} = \frac{\partial}{\partial t} + \mathbf{v} \cdot \nabla$ denotes a substantive (material) derivative associated with the vector field $\mathbf{v} : \Omega \times [0, \infty) \rightarrow \mathbb{R}^3$. The expression $\rho \frac{Dv_\alpha}{Dt}$ for the rate of momentum change is as basic as the general assumptions of continuum media mechanics, but the form of expression of forces acting on the fluid element require further assumptions. The standard approach is that for any continuum, forces acting on a piece of material are of two types: (i) forces of stress where piece of material is acted on by forces across its surface by the rest of a body; (ii) external (body) forces such as gravity, electromagnetic, or centrifugal force.

It is a common practice to highlight the contribution due to the surface forces as separate terms in the momentum equation and to include the effects of body forces as source terms.

The surface part of forces (stress) can be described by the pressure (scalar) and nine viscous stress components (tensor): p and $\tau = [\tau_{\alpha\beta}]$, where $\alpha, \beta \in \{x, y, z\}$. The meaning of stress components is as follows: $\tau_{\alpha\beta}$ = the stress component acting in the α - direction on a surface normal to the β - direction. Now we can write the momentum equations as

$$\rho \frac{Dv_\alpha}{Dt} = -\frac{\partial p}{\partial \alpha} + \frac{\partial \tau_{x\alpha}}{\partial x} + \frac{\partial \tau_{y\alpha}}{\partial y} + \frac{\partial \tau_{z\alpha}}{\partial z} + B_\alpha \quad \text{for } \alpha = x, y, z. \quad (3)$$

In the above equation the effects of surface stresses are shown explicitly while the body forces are contained in the source terms B_x, B_y, B_z . As an example we can write for the gravitational force near the earth surface (where homogeneous gravity can be assumed) $B_x = B_z = 0$ and $B_z = -\rho g$.

Energy equation

Basically this fundamental law is embodied in the first law of thermodynamics which states that the rate of change of energy of a fluid element is equal to the rate of heat input plus the rate of work done on that element:

$$\left[\begin{array}{c} \text{rate of change} \\ \text{of energy of an element} \end{array} \right] = \left[\begin{array}{c} \text{net rate of heat} \\ \text{input to the element} \end{array} \right] + \left[\begin{array}{c} \text{net rate of work done} \\ \text{on the element} \end{array} \right]$$

The rate of work done on the media element by surface forces equals to the product of force and velocity component in the force direction. Taking into consideration the pressure field and stress tensor introduced earlier we can arrive at the following equation for the work rate by forces in the x -direction

$$-\frac{\partial(pv_x)}{\partial x} + \frac{\partial(v_x \tau_{xx})}{\partial x} + \frac{\partial(v_x \tau_{yx})}{\partial y} + \frac{\partial(v_x \tau_{zx})}{\partial z}. \quad (4)$$

Analogous expressions hold for components y and z .

The next contribution to energy balance is connected with the heat flux \mathbf{J}^q . The net heat transfer per unit volume into the element due to heat flow is given by $-\text{div} \mathbf{J}^q$. If Fourier's law of heat conduction is applicable, then $\mathbf{J}^q = -\kappa \nabla T$ so we get $-\text{div}(\kappa \nabla T)$. Here $\kappa > 0$ denotes the thermal conductivity. Taking into account all these contributions and the source of energy S_E leads to the following energy balance equation

$$\rho \frac{DE}{Dt} = -\text{div}(p\mathbf{v}) + \left(\frac{\partial(v_x \tau_{xx})}{\partial x} + \frac{\partial(v_x \tau_{yx})}{\partial y} + \frac{\partial(v_x \tau_{zx})}{\partial z} + \frac{\partial(v_y \tau_{xy})}{\partial x} + \frac{\partial(v_y \tau_{yy})}{\partial y} + \frac{\partial(v_y \tau_{zy})}{\partial z} + \frac{\partial(v_z \tau_{xz})}{\partial x} + \frac{\partial(v_z \tau_{yz})}{\partial y} + \frac{\partial(v_z \tau_{zz})}{\partial z} \right) + \text{div}(\kappa \nabla T) + S_E, \quad (5)$$

where energy density $E = u + \frac{1}{2}(v_x^2 + v_y^2 + v_z^2)$ with u the internal energy density.

Although equation (5) is proper energy balance it is usually not used in this form. Rather we rewrite it in such way that kinetic and internal energies are separated. This requires to develop the expression for the term $\frac{D\left(\frac{1}{2}(v_x^2 + v_y^2 + v_z^2)\right)}{Dt}$. It can be achieved by multiplying the momentum equation (3) by the velocity component v_α and adding the results for

$\alpha = x, y, z$. After some algebra we arrive at the equation for the internal energy u :

$$\rho \frac{Du}{Dt} = -p \operatorname{div} v + \operatorname{div}(\kappa \nabla T) + \sum_{\alpha, \beta} \tau_{\alpha\beta} \frac{\partial v_\beta}{\partial \alpha} + S_i, \quad (6)$$

where the source term is now defined as $S_i = S_E - v \cdot B$ with body forces introduced earlier (the momentum equation (3)).

In a special but important case of an incompressible fluid we have $u = c_p T$ and $\operatorname{div} v = 0$, where c_p is the specific heat. Now the equation (6) can be written for temperature as follows

$$\rho c_p \frac{DT}{Dt} = \operatorname{div}(\kappa \nabla T) + \sum_{\alpha, \beta} \tau_{\alpha\beta} \frac{\partial v_\beta}{\partial \alpha} + S_i. \quad (7)$$

On the other hand, for compressible flows the equation (6) is usually written in the form for the enthalpy. The specific enthalpy h and the specific total enthalpy h_0 are defined as

$$h = u + \frac{\rho}{p}, \quad h_0 = h + \frac{1}{2}(v_x^2 + v_y^2 + v_z^2),$$

what combined with the definition of specific energy $E = u + \frac{1}{2}(v_x^2 + v_y^2 + v_z^2)$ gives the total enthalpy equation

$$\frac{\partial(\rho h_0)}{\partial t} + \operatorname{div}(\rho h_0 v) = \operatorname{div}(\kappa \nabla T) + \frac{\partial p}{\partial t} + \sum_{\alpha, \beta} \frac{\partial(v_\beta \tau_{\alpha\beta})}{\partial \alpha} + S_i. \quad (8)$$

Let Ω be a region in \mathbb{R}^3 and $T(x, t)$ temperature at point $x \in \Omega$ and time $t \geq 0$. The special case of (7) – the conservation of thermal energy – leads to the equation

$$c_p \rho \frac{\partial T}{\partial t} = \operatorname{div}(\kappa \nabla T), \quad (9)$$

where c_p – the specific heat (thermal capacity), ρ – the density (mass per unit volume), κ – the thermal conductivity. If all these coefficients are constant, then equation takes the form

$$\frac{\partial T}{\partial t} = \theta \Delta T, \quad (10)$$

where $\theta = \kappa/c_p \rho$ is the so called thermal diffusivity.

In the case of the axial symmetry the equation (10) can be written as

$$\frac{\partial T}{\partial t} = \theta \left(\frac{\partial^2 T}{\partial r^2} + \frac{1}{r} \frac{\partial T}{\partial r} + \frac{1}{r^2} \frac{\partial^2 T}{\partial \phi^2} \right), \quad (11)$$

where the temperature field is expressed in the cylindrical coordinates $T = T(r, \phi, t)$.

The equation must be supplemented by appropriate side conditions such as the initial temperature $T_0 : \Omega \rightarrow \mathbb{R}$, i.e.

$$T(x, 0) = T_0(x) \quad x \in \Omega, \quad (12)$$

and boundary condition: Dirichlet if the temperature is controlled on the boundary $\partial\Omega$, Neumann if the heat flow across $\partial\Omega$ is controlled, or Robin type if the flow obeys Newton's law of cooling. In the case of temperature control over the boundary we have formal statement as

$$T(x, t) = g(x, t) \quad \text{for } x \in \partial\Omega, \quad t \geq 0, \quad (13)$$

where the function $g : \partial\Omega \times [0, \infty) \rightarrow \mathbb{R}$ (temperature distribution on the boundary) is given. In the case of heat flow according to Newton's law the boundary condition (called also the Robin boundary condition) reads

$$-\kappa \frac{\partial T}{\partial n}(x, t) = h(T(x, t) - T_a(t)) \quad \text{for } x \in \partial\Omega, \quad t \geq 0, \quad (14)$$

where $h > 0$ – the heat transfer (exchange) coefficient, $T_a(t)$ – the ambient temperature. Here the symbol $\frac{\partial T}{\partial n}$ means the derivative in the normal direction at the boundary points. This may also be expressed as following: $\frac{\partial T}{\partial n} = (\nabla T) \cdot n$, where $n : \partial\Omega \rightarrow \mathbb{R}^3$ is the normal vector field on the boundary, i.e. (a) unit length, $|n(x)| = 1$, (b) $n(x)$ is perpendicular to the boundary at $x \in \partial\Omega$, (c) $n(x)$ points in the outward direction.

3. Numerical method

There are three main categories of numerical techniques in the heat transport problems: finite difference, finite element, and spectral methods [7]. We will use the FLUENT environment which is based on the *finite volume method* – a special type of the finite difference method [7]. The numerical treatment consists of the following steps: (1) integration of the equations over all the control volumes of the domain, (2) discretization or conversion of the resulting integral equations into system of algebraic equations, (3) solution of the algebraic equations (usually by some iterative method).

The basic steps of finite volume discretization

As can be seen from the previous section – esp. equations (2), (3), and (7) – the conservative (divergence) form of the equations which govern the time-dependent fluid flow and heat transfer can be written in the following generic way

$$\frac{\partial(\rho\varphi)}{\partial t} + \operatorname{div}(\rho\varphi u) = \operatorname{div}(\theta \nabla \varphi) + S(\varphi), \quad (15)$$

where φ is the any conserved quantity (mass fraction of a chemical species, component of velocity (momentum equation), the enthalpy or temperature (energy) etc.), $u = (u_x, u_y, u_z)$ is the vector field of velocities, $\theta > 0$ is diffusion coefficient, and $S(\varphi)$ is the source term. The quantities are θ and S are specific to a particular meaning of φ .

Step1: Equation (15) is the starting point of numerical procedure based on the *finite volume method*. The key step of this approach is the integration of (15) over a control volume $C \subset \mathbb{R}^3$:

$$\int_C \frac{\partial(\rho\varphi)}{\partial t} dx + \int_C \operatorname{div}(\rho\varphi u) dx = \int_C \operatorname{div}(\theta \nabla \varphi) dx + \int_C S(\varphi) dx, \quad (16)$$

where dx denotes integration with respect to the volume measure in space. Applying now the Gauss's divergence theorem, $\int_C \operatorname{div}(v) dx = \int_{\partial C} n \cdot v da$, the above equality takes the form

$$\frac{\partial}{\partial t} \int_C \rho\varphi dx + \int_{\partial C} n \cdot (\rho\varphi u) da = \int_{\partial C} n \cdot (\theta \nabla \varphi) da + \int_C S(\varphi) dx. \quad (17)$$

In a steady state case there is no time dependence and eq. (17) is

$$\int_{\partial C} n \cdot (\rho \varphi u) da = \int_{\partial C} n \cdot (\theta \nabla \varphi) da + \int_C S(\varphi) dx, \quad (18)$$

what has a clear interpretation as flux balance in the control volume C : the left side gives the total flux across the boundary ∂C and the right side contains the diffusive flux and the source (production or consumption) of the property φ in the volume C .

In time-dependent problems it is necessary to integrate over small time interval $[t, \Delta t]$ what gives the following most general integrated form of the transport equation in finite volume method:

$$\left(\int_C \rho \varphi dx \right) \Big|_t^{t+\Delta t} + \int_t^{t+\Delta t} \int_{\partial C} n \cdot (\rho \varphi u) da = \int_t^{t+\Delta t} \int_{\partial C} n \cdot (\theta \nabla \varphi) da + \int_t^{t+\Delta t} \int_C S(\varphi) dx. \quad (19)$$

Step 2: Divide the domain into small control volumes centered around nodal points. Usually control volume near the boundary of the domain are set up in such a manner that the physical boundary coincide with the part of control volume boundary.

Step 3: Apply some form of approximation to integrals in equations (18) or (19) which will be expressed by the values of unknown conserved quantity φ at nodal points (for volume integrals, $\int_C (\dots) dx$), and values of fluxes of φ at the faces (for surface integrals $\int_{\partial C} (\dots) da$).

Step 4: Solution of the resulting system of linear algebraic equations which gives the distribution of φ at nodal points. In practical situations (2D or 3D geometry) we obtain large systems so direct methods (such as Gauss elimination, LU decomposition etc.) are not suitable. Generally iterative methods for solving such systems are utilized (Gauss-Seidel or multi-grid techniques) [7], [8].

4. Numerical solutions for 3D geometry

Computer simulations of temperature distributions were carried out using FLUENT package. Results for several geometries, different initial and boundary conditions, and thermal properties at selected times are shown – see **Figure 1 - Figure 3**.

In **Figure 1** steady-state temperature distribution in four phase system is presented. Different views are displayed (3D and cross-sections). Calculations have been performed for the following data: 1) thermal diffusivities of materials: $\theta_{M1} = 4.03 \cdot 10^{-6} \text{ m}^2 \cdot \text{s}^{-1}$, $\theta_{M3} = 1.19 \cdot 10^{-4} \text{ m}^2 \cdot \text{s}^{-1}$, $\theta_{M4} = 2.82 \cdot 10^{-6} \text{ m}^2 \cdot \text{s}^{-1}$, 2) initial temperature in the whole volume $T(x, 0) = 300 \text{ K}$, 3) boundary conditions: adiabatic at the side surface of the cylinder M1, Dirichlet boundary condition (13) – uniform temperature 350 K at the bottom and Neumann boundary conditions $J = 1000 \text{ W} \cdot \text{m}^{-2}$ on the top wall. Calculations for two different thermal conductivities of the M2 rod: $\kappa_{M2} = 202.4 \text{ W} \cdot \text{m}^{-1} \cdot \text{K}^{-1}$ – left column, $\kappa_{M2} = 20.24 \text{ W} \cdot \text{m}^{-1} \cdot \text{K}^{-1}$ – right column are presented in **Figure 1**.

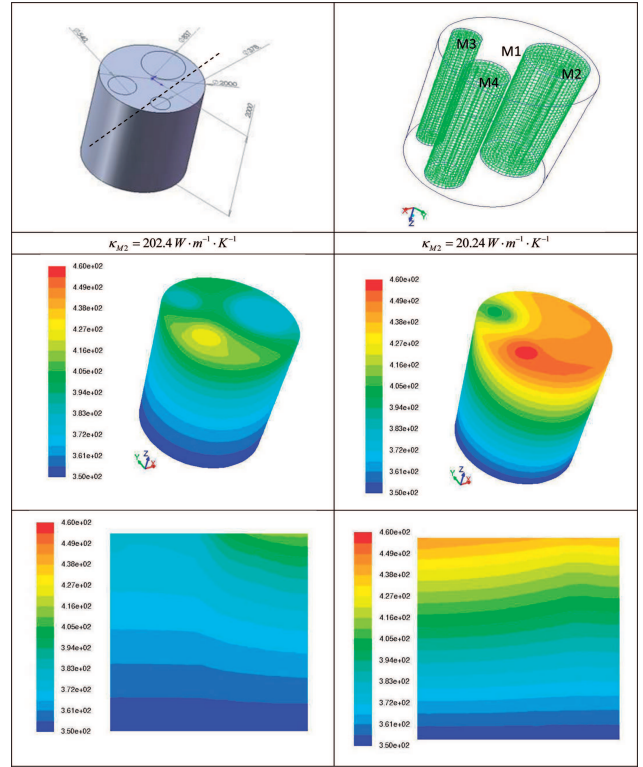


Fig. 1. Steady-state temperature distribution. Rods made of materials denoted by M2, M3 and M4 are plunged in the cylinder M1. Thermal diffusivities of materials are as follows: $\theta_{M1} = 4.03 \cdot 10^{-6} \text{ m}^2 \cdot \text{s}^{-1}$, $\theta_{M3} = 1.19 \cdot 10^{-4} \text{ m}^2 \cdot \text{s}^{-1}$, $\theta_{M4} = 2.82 \cdot 10^{-6} \text{ m}^2 \cdot \text{s}^{-1}$. Initial temperature in the whole volume $T(x, 0) = 300 \text{ K}$. Boundary conditions adiabatic at the side surface of cylinder M1, Dirichlet boundary condition 350 K at the bottom and Neumann boundary condition $J = 1000 \text{ W} \cdot \text{m}^{-2}$ on the top wall. Calculations for two different thermal conductivities of the M2 rod: $\kappa_{M2} = 202.4 \text{ W} \cdot \text{m}^{-1} \cdot \text{K}^{-1}$ – left column, $\kappa_{M2} = 20.24 \text{ W} \cdot \text{m}^{-1} \cdot \text{K}^{-1}$ – right column

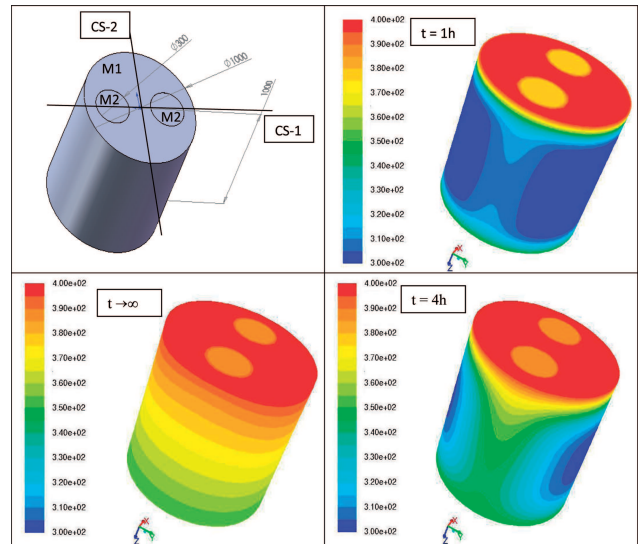


Fig. 2. Geometry of 3D object case 2. Cylinders made of materials denoted as M2 are plunged in the cylinder M1. Thermal properties of materials are as follows: $\theta_{M1} = 8.43 \cdot 10^{-7} \text{ m}^2 \cdot \text{s}^{-1}$, $\theta_{M2} = 4.03 \cdot 10^{-6} \text{ m}^2 \cdot \text{s}^{-1}$. Initial temperature in the whole volume $T(x, 0) = 300 \text{ K}$. Adiabatic boundary conditions at the side surface of the cylinder M1, Dirichlet boundary condition at the bottom 350 K and Robin boundary conditions $h = 1000 \text{ W} \cdot \text{m}^{-2} \cdot \text{K}^{-1}$, $T_a = 400 \text{ K}$ on the top wall

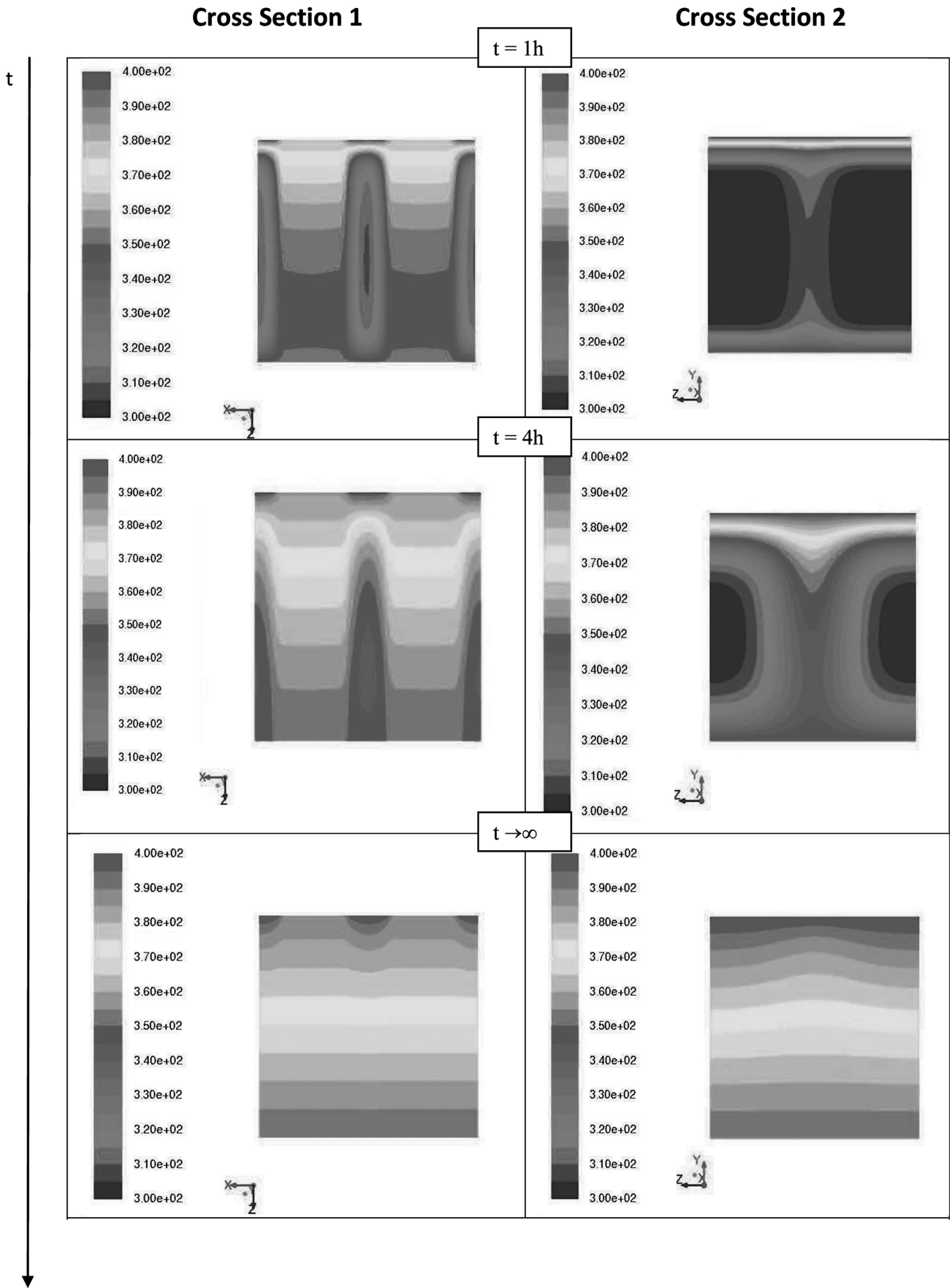


Fig. 3. Temperature distribution for cross-sections 1 and 2 from Figure 2 at selected times

In **Figure 2** and **Figure 3** temperature distributions for selected times: $1h$, $4h$, and $t \rightarrow \infty$ are shown. Calculations have been performed for the following data: 1) thermal diffusivities of materials: $\theta_{M1} = 4.03 \cdot 10^{-6} m^2 \cdot s^{-1}$, $\theta_{M2} = 8.55 \cdot 10^{-5} m^2 \cdot s^{-1}$, 2) initial temperature in the whole volume $T(x, 0) = 300 K$, 3) boundary conditions: adiabatic at the side surface of the cylinder M1, Dirichlet boundary condition (13) – uniform temperature $350 K$ at the bottom and Robin boundary conditions (14) on the top wall ($h = 1000 W \cdot m^{-2} \cdot K^{-1}$, $T_a(t) = 400 K$). 3D views for selected times are displayed in **Figure 2** and the corresponding cross-sections in **Figure 3**.

5. Analytical solutions

Example 1 (one phase analytical solution)

Let us consider the following set of equations

$$\begin{cases} \frac{\partial T}{\partial t} = \theta \frac{\partial^2 T}{\partial x^2} & \text{for } 0 < x < d, t > 0, \\ T(0, t) = T_L, & -\kappa \frac{\partial T}{\partial x}(d, t) = J_R, \\ T(x, 0) = T_0, \end{cases} \quad (20)$$

which describes the heat conduction of a one-dimensional rod with the boundary conditions: constant temperature T_L kept at left side, $x = 0$, and constant feed of heat J_R at the right side, $x = d$.

By simple change of variable, $\tilde{T}(x, t) := T(x, t) - [T_L - \frac{J_R}{\kappa}x]$, this set is easily converted into the following homogeneous problem

$$\begin{cases} \frac{\partial \tilde{T}}{\partial t} = \theta \frac{\partial^2 \tilde{T}}{\partial x^2} & \text{for } 0 < x < d, t > 0, \\ \tilde{T}(0, t) = 0, & \frac{\partial \tilde{T}}{\partial x}(d, t) = 0, \\ \tilde{T}(x, 0) = T_0 - T_L + \frac{J_R}{\kappa}x. \end{cases} \quad (21)$$

The solution may be obtained by the separation of variables method in which we seek the building blocks of the solution in the form of the functions $T_k(t)X_k(x)$. This leads to the following expression

$$T(x, t) = T_L - \frac{J_R}{\kappa}x + \sum_{k=0}^{\infty} A_k e^{-\lambda_k^2 t} \sin\left((k + \frac{1}{2})\pi \frac{x}{d}\right), \quad (22)$$

where $\lambda_k = (k + \frac{1}{2})\frac{\pi\sqrt{\theta}}{2d}$, $k = 0, 1, 2, \dots$. The coefficients A_k in the formula (22) are calculated as the sine Fourier series coefficients

$$A_k = \frac{2}{d} \int_0^d \sin\left((k + \frac{1}{2})\frac{\pi x}{d}\right) \tilde{T}(x, 0) dx \quad \text{for } k = 0, 1, 2, \dots \quad (23)$$

In the particular application of (23) to initial conditions of the problem (21) we arrive after some algebra at

$$A_k = \frac{2(T_0 - T_L)}{(k + \frac{1}{2})\pi} + \frac{2J_R d}{\kappa \pi^2} \frac{(-1)^k}{(k + \frac{1}{2})^2}, \quad k = 0, 1, 2, \dots \quad (24)$$

$$T(x, t) = \begin{cases} T_L + \frac{2(\xi(t) - T_L)}{d}x + \sum_{k=1}^{\infty} A_k e^{-(2k\pi/d)^2 \theta_1 t} \sin \frac{2k\pi x}{d} & \text{for } 0 \leq x \leq \frac{1}{2}d, \\ \xi(t) + \frac{2(T_R - \xi(t))}{d}(x - \frac{d}{2}) + \sum_{k=1}^{\infty} A_k e^{-(2k\pi/d)^2 \theta_2 t} \sin \frac{2k\pi(x - \frac{1}{2}d)}{d} & \text{for } \frac{1}{2}d \leq x \leq d, \end{cases} \quad (26)$$

The example calculations – solution of heat transport at selected times are presented in **Figure 4**. Next **Figure 5** compares different methods (tools): analytical solution, method of lines – MATLAB implementation, and finite volume method – ANSYS FLUENT. All three methods give the same results with the relative error less than 1%.

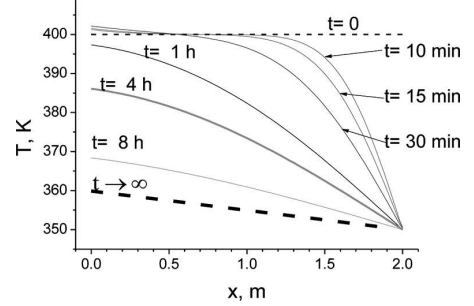


Fig. 4. Evolutional solution of heat transport for a single phase 1D geometry for mixed boundary conditions – problem (20). Dashed lines represent initial temperature $400 K$ – thin line and steady state solution $t \rightarrow \infty$ – thick line

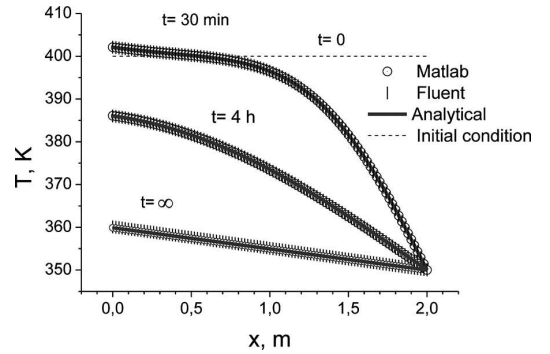


Fig. 5. Solution of heat transport for a single phase 1D geometry for mixed boundary conditions – problem (20). Comparison of different methods, tools: 1) analytical solution, 2) method of lines – MATLAB, finite volume method – ANSYS FLUENT

Example 2 (two phase analytical solution)

One dimensional rod has non-constant conductivity coefficient. Specifically we assume that the first half has conductivity θ_1 and for the second it is θ_2 . Both ends are kept at constant temperature (Dirichlet boundary condition). This system may be described by the following equations

$$\begin{cases} \frac{\partial T_1}{\partial t} = \theta_1 \frac{\partial^2 T_1}{\partial x^2} & (0 < x < \frac{1}{2}d), & \frac{\partial T_2}{\partial t} = \theta_2 \frac{\partial^2 T_2}{\partial x^2} & (\frac{1}{2}d < x < d), \\ T_1(\frac{1}{2}d, t) = T_2(\frac{1}{2}d, t), & \kappa_1 \frac{\partial T_1}{\partial x}(\frac{1}{2}d, t) = \kappa_2 \frac{\partial T_2}{\partial x}(\frac{1}{2}d, t), \\ T_1(0, t) = T_L, & T_2(d, t) = T_R, \\ T(x, 0) = T_0, \end{cases} \quad (25)$$

The analytical solution to this problem can be written as

where the time-dependent function $\xi(t)$ is defined as

$$\xi(t) = \frac{T_L \kappa_1 + T_R \kappa_2}{\kappa_1 + \kappa_2} + \frac{\pi}{\kappa_1 + \kappa_2} \sum_{k=1}^{\infty} k A_k \left(\kappa_2 e^{(2k\pi/d)^2 \theta_2 t} - (-1)^k \kappa_1 e^{(2k\pi/d)^2 \theta_1 t} \right) \quad \text{for } t > 0, \quad (27)$$

and coefficients A_k are given by the formula similar to (23).

The example calculations – temperature distributions in the two phase system for the problem (25) at several times are presented below – **Figure 6**. Solution of the heat trans-

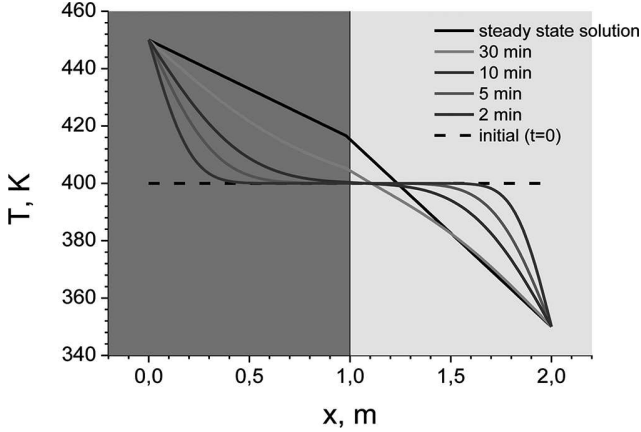


Fig. 6. Solution of the heat transport for two phase 1D geometry – problem(25) – the following data were used:

$$\theta = 8.55 \cdot 10^{-5} \text{ m}^2 \cdot \text{s}^{-1}, \quad (\kappa = 202.4 \text{ W} \cdot \text{m}^{-1} \cdot \text{K}^{-1}), \theta = 1.13 \cdot 10^{-4} \text{ m}^2 \cdot \text{s}^{-1}, \quad (\kappa = 387.6 \text{ W} \cdot \text{m}^{-1} \cdot \text{K}^{-1}), T_L = 450 \text{ K}, T_R = 350 \text{ K}$$

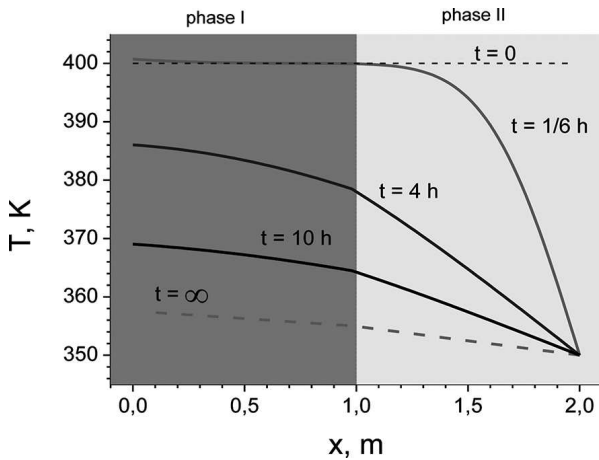


Fig. 7. Evolutional solution of heat transport for 1D geometry for two phase system – problem (25) and mixed (Dirichlet –right boundary and Neumann –left boundary conditions) the following data were used: $\theta = 8.55 \cdot 10^{-5} \text{ m}^2 \cdot \text{s}^{-1}$, $(\kappa = 202.4 \text{ W} \cdot \text{m}^{-1} \cdot \text{K}^{-1})$, $\theta = 1.13 \cdot 10^{-4} \text{ m}^2 \cdot \text{s}^{-1}$, $(\kappa = 387.6 \text{ W} \cdot \text{m}^{-1} \cdot \text{K}^{-1})$, $J_L = 1000 \text{ W} \cdot \text{m}^{-2}$, $T_R = 350 \text{ K}$. Dashed lines represent initial temperature 400 K – thin line and steady state solution $t \rightarrow \infty$ – thick line

port problem but for mixed boundary conditions (Dirichlet and Neumann) are demonstrated in Figure 7.

In **Figure 8** the heat transport solutions for one- and two-phase systems are compared. Clearly one can see on the plot a discontinuity of the temperature gradient (temperature profile is not smooth at one point) due to the continuity of the heat flux (cf. (28)) in the case of two phase system.

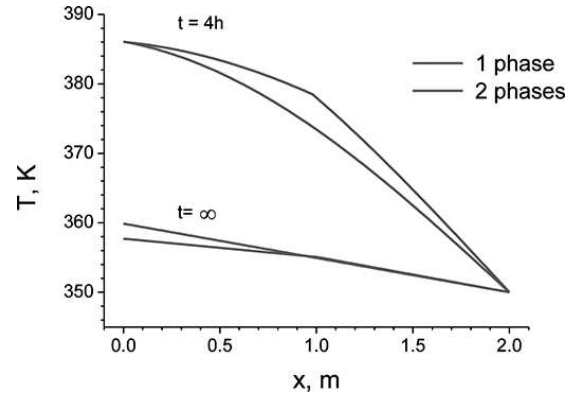


Fig. 8. Evolutional solution of heat transport for 1D geometry for mixed (Dirichlet at left boundary and Neumann at right boundary conditions). Comparison of solutions for one phase – problem (20) and for two phase – problem (25) systems. Clearly we can see on the plot a discontinuity of the temperature gradient (temperature profile is not smooth at one point) due to the continuity of the heat flux (cf. (28))

6. Inverse problems

Example 3 (1D inverse problem)

In this two-phase one dimensional heat problem the thickness of one phase is not known. In other words the position $\ell \in (0, d)$, where two phases meet, is unknown. Formally the problem can be described by the following set of equations

$$\begin{cases} \frac{\partial T_1}{\partial t} = \theta_1 \frac{\partial^2 T_1}{\partial x^2} & (0 < x < \ell), & \frac{\partial T_2}{\partial t} = \theta_2 \frac{\partial^2 T_2}{\partial x^2} & (\ell < x < d), \\ T_1(\ell, t) = T_2(\ell, t), & \kappa_1 \frac{\partial T_1}{\partial x}(\ell, t) = \kappa_2 \frac{\partial T_2}{\partial x}(\ell, t), \\ T_1(0, t) = T_L, & T_2(d, t) = T_R, \\ T(x, 0) = T_0. \end{cases} \quad (28)$$

The analytical solution of the problem (28) is given by

$$T(x, t; \ell) = \begin{cases} T_L + \frac{\xi(\ell, t) - T_L}{\ell} x + \sum_{k=1}^{\infty} A_k e^{-(k\pi/\ell)^2 \theta_1 t} \sin \frac{k\pi x}{\ell} & \text{for } 0 \leq x \leq \ell, \\ \xi(\ell, t) + \frac{T_R - \xi(\ell, t)}{(d-\ell)} (x - \ell) + \sum_{k=1}^{\infty} A_k e^{-(k\pi/(d-\ell))^2 \theta_2 t} \sin \frac{k\pi(x-\ell)}{d-\ell} & \text{for } \ell \leq x \leq d, \end{cases} \quad (29)$$

where

$$\xi(\ell, t) = \frac{\kappa_1 T_L (d-\ell) + \kappa_2 T_R \ell}{\kappa_1 (d-\ell) + \kappa_2 \ell} + \frac{\pi \ell (d-\ell)}{\kappa_1 (d-\ell) + \kappa_2 \ell} \sum_{k=1}^{\infty} k \left(\kappa_2 A_{2,k} e^{(2k\pi/(d-\ell))^2 \theta_2 t} - (-1)^k \kappa_1 A_{1,k} e^{(2k\pi/\ell)^2 \theta_1 t} \right) \quad t > 0, \quad (30)$$

$$A_{1,k} = \frac{2T_0}{\ell} \int_0^{\ell} \sin \left(\left(k + \frac{1}{2} \right) \frac{\pi x}{\ell} \right) dx, \quad A_{2,k} = \frac{2T_0}{d-\ell} \int_{\ell}^d \sin \left(\left(k + \frac{1}{2} \right) \frac{\pi x}{d-\ell} \right) dx \quad \text{for } k = 0, 1, 2, \dots$$

At steady state, i.e. for $t \rightarrow \infty$, we have

$$T(x; \ell) = \lim_{t \rightarrow \infty} T(x, t; \ell) = \begin{cases} T_L + \frac{\xi(\ell) - T_L}{\ell} x & \text{for } 0 \leq x \leq \ell, \\ \xi(\ell) + \frac{T_R - \xi(\ell)}{(d - \ell)} (x - \ell) & \text{for } \ell \leq x \leq d, \end{cases} \quad (31)$$

where

$$\xi(\ell) = \frac{\kappa_1 T_L (d - \ell) + \kappa_2 T_R \ell}{\kappa_1 (d - \ell) + \kappa_2 \ell},$$

and putting both expressions together we obtain

$$T(x; \ell) = \begin{cases} T_L + \frac{\kappa_2 (T_R - T_L)}{\kappa_1 (d - \ell) + \kappa_2 \ell} x & \text{for } 0 \leq x \leq \ell, \\ \frac{\kappa_1 T_L (d - \ell) + \kappa_2 T_R \ell}{\kappa_1 (d - \ell) + \kappa_2 \ell} + \frac{\kappa_1 T_R - \kappa_2 T_L}{\kappa_1 (d - \ell) + \kappa_2 \ell} (x - \ell) & \text{for } \ell \leq x \leq d. \end{cases} \quad (32)$$

If we now know the stationary value of temperature T^* at some point $x^* \in (\ell, d)$, then we can easily find the parameter ℓ by solving the equation $T(x^*; \ell) = T^*$ which according to (32) takes the form

$$\frac{\kappa_1 T_L (d - \ell) + \kappa_2 T_R \ell}{\kappa_1 (d - \ell) + \kappa_2 \ell} + \frac{\kappa_1 T_R - \kappa_2 T_L}{\kappa_1 (d - \ell) + \kappa_2 \ell} (x^* - \ell) = T^*. \quad (33)$$

As the equation has a unique solution for any $T^* \in (T_L, T_R)$ so the inverse problem in this simple case leads to a well-posed problem.

Example 4 (the inverse problem – 3D case)

This example presents the formulation of the problem of estimating the refractory lining inner profile of a blast furnace crucible based on the measurement of temperatures at selected locations [9]. The measured values are used to assess the shape of the lining curve by means of the inverse problem founded on the heat transfer equations and boundary conditions. However, this problem is somewhat atypical as parameters that we look for is the shape of a part of the boundary. In other words the region $\Omega \subset \mathbb{R}^3$ is unknown and must be determined. Thus we have $\Omega_{(P_1, \dots, P_m)}$ where $P_1, \dots, P_m \in \mathbb{R}^2$ are unknown points on the plane which describe part of the boundary $\partial\Omega$. Now the formulation is as follows. Let us define the error function

$$err(t; P_1, \dots, P_m) = \sum_{i=1}^N (T(t, x_i; P_1, \dots, P_m) - T_{i,t}^*)^2 \quad (34)$$

where $\{x_i\}_{i=1}^N \subset \Omega_{(P_1, \dots, P_m)}$ are points where the temperatures measured, $T_{i,t}^*$ are values of the measured temperatures at time $t > 0$. The standard procedure is now to require the error function (34) to take minimum value. Thus, we look for P_1^*, \dots, P_m^* such that

$$err(t; P_m^*, \dots, P_1^*) = \min_{P_1, \dots, P_m} err(t; P_1, \dots, P_m) = \min_{P_1, \dots, P_m} \sum_{i=1}^N (T(t, x_i; P_1, \dots, P_m) - T_{i,t}^*)^2, \quad (35)$$

where $T(t, x; P_1, \dots, P_m)$ is the solution of the following problem

$$\begin{cases} \frac{\partial T}{\partial t}(x, t) = \theta \Delta_x T(x, t), & x \in \Omega_{(P_1, \dots, P_m)}, \quad t \geq 0, \\ T(x, 0) = T_0(x), & x \in \Omega_{(P_1, \dots, P_m)}, \quad T(x, t) = g(x), \quad x \in \partial\Omega_{(P_1, \dots, P_m)}. \end{cases} \quad (36)$$

The boundary conditions in the problem (36) do not have to be of pure Dirichlet type. In fact we used mixed conditions in the exemplary calculations for the case shown in **Figure 9**. The geometry of the inner part of the pot may change but only in such way that the thickness of the inner layer is changing. Thus the shape is basically the same and Ω_d depends only on one parameter $d \in [10 \text{ cm}, 30 \text{ cm}]$. The number of temperature measurement was $N = 6$ at steady state (in the above formulation (35), (36) it means that $t \rightarrow \infty$). Thus the error function (35) in the consider case is one dimensional, $err(d) \in \mathbb{R}_+$. Its plot is in the first row, second column of **Figure 9** and we see that there is a clear global minimum. In other words had we tried to assess the thickness of the pot by taking measurements as indicated in **Figure 9** at $N = 6$ points and employed any valid optimization procedure for the inverse problem we would have recovered this thickness from temperature measurements.

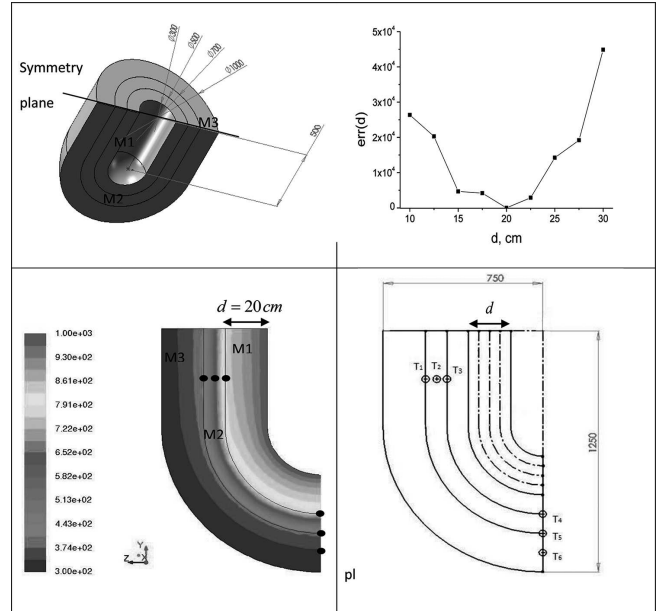


Fig. 9. 3D inverse problem calculations. Layers of materials denoted as outside M1, inner M2 and inside steel M3. Thermal properties of materials are as follows: $\kappa_{M1} = 19.00W \cdot m^{-1} \cdot K^{-1}$, $\kappa_{M2} = 2.25W \cdot m^{-1} \cdot K^{-1}$, $\kappa_{M3} = 16.27W \cdot m^{-1} \cdot K^{-1}$. Initial temperature in the whole volume $T(x, 0) = 400 \text{ K}$. Adiabatic boundary conditions at the top. Dirichlet boundary condition at the inner wall and Robin boundary conditions $h = 1000 \text{ W} \cdot m^{-2} \cdot K^{-1}$, $T_a = 300 \text{ K}$ on the outer wall

7. Summary

One- and two-dimensional problems involving heat transfer phenomena can be relatively easily handled using self-made non-commercial programs. But real world – industrial problems usually require full 3D modeling. This cannot be achieved easily in all generality without resorting to powerful, flexible and versatile commercial computational software. There are many such products like: ABQUS, COMSOL, ALGOR, COMET, STAR CD and FLUENT, etc. We have chosen ANSYS FLUENT CFD package to perform simulations and tests which is available in the Academic Computer Centre CYFRONET AGH [10].

The main goal of the paper was to present various simulations of heat transfer phenomena and possible use of the inverse problems in this area. We have also advocated the use of special cases where analytical solutions could be obtained as a tool for testing.

We have carried out calculations of the temperature distribution for several examples: steady and evolutionary states, both for single and multiphase systems for 1D and 3D geometries. The results obtained from FLUENT and by using independent numerical procedure based on the method of lines led to very good agreement with the analytical solutions for 1D geometry. Formulation of special inverse problems for heat equation in 1D and 3D geometries was given. Analytical solution of the steady-state inverse problem in 1D geometry was presented. In the case of 3D geometry the error function was calculated using FLUENT exhibiting one global minimum. This idea will be developed in future research by incorporating more complicated shape optimization via the inverse method for industrial applications.

Acknowledgments

This work has been supported in part by AGH grant, PL-Grid infrastructure and the Academic Computer Centre CYFRONET AGH.

Appendix

Method of lines for 1D non-steady case

The method of lines [11] will be employed to solve numerically the PDE system describing non-stationary heat transport in 1D geometry with mixed Dirichlet and Neumann boundary conditions(13), (14). An uniform grid is used. The temperature is defined at points y_k while the heat fluxes at points x_k (Figure 10). Each point y_k is placed in the middle of the interval $[x_{k+1}, x_k]$ hence $y_k = \frac{1}{2}(x_{k+1} + x_k)$.

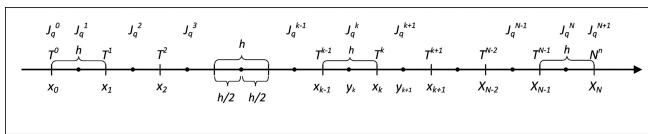


Fig. 10. Space grid for heat transport problem

The finite difference approximation of non-stationary heat transport equation which corresponds to the above grid for internal nodes reads

$$\frac{dT^k}{dt}(t) := \frac{\partial T}{\partial t}(y_k, t) = -\frac{\partial J_q}{\partial x}(y_k, t) \approx -\frac{J_q(x_{k+1}, t) - J_q(x_k, t)}{h} = \frac{J_q^{k+1}(t) - J_q^k(t)}{h},$$

$$J_q^k(t) = J_q(x_k, t) = -\lambda \frac{\partial T}{\partial x}(x_k, t) \approx -\lambda \frac{T^k - T^{k-1}}{h}$$

for $k = 1, \dots, N-1$.

(37)

and for boundary nodes the one-sided non-uniform finite differences (Appendix 1) are used

$$\frac{dT^0}{dt} = 0 \quad (\text{Dirichlet b.c.}),$$

$$\frac{dT^{N+1}}{dt} = \frac{J_q^{N-1}(t) - 4J_q^N(t) + 3J_q^{N+1}(t)}{h} = \frac{J_q^{N-1}(t) - 4J_q^N(t) + 3J_R}{h} \quad (\text{Neumann b.c.}),$$

(38)

where $J_q^{N+1}(t) = J_R$ (Neumann boundary condition).

Equations (37) and (38) together with initial conditions lead to initial ODEs problem (Cauchy problem):

$$\begin{cases} \frac{dT^1}{dt} = -\lambda \frac{T^2 - 2T^1 + T_L}{h^2}, \\ \vdots \\ \frac{dT^k}{dt} = -\lambda \frac{T^{k+1} - 2T^k + T^{k-1}}{h^2} \quad \text{for } k = 2, \dots, N, \\ \vdots \\ \frac{dT^{N+1}}{dt} = -\lambda \frac{T^{N-1} - 3T^N + 4T^{N+1}}{h^2}, \\ T^k(0) = T_0 \quad \text{for } k = 1, \dots, N+1 \end{cases} \quad (39)$$

Steady state case

Steady state solution can be find two different ways:

- 1) as an asymptotic solution of non-steady state solution and
- 2) directly as a solution of steady state formulation. Steady state formulation for a heat transport in the example one – eq. (20) – takes a form:

$$\begin{cases} \frac{\partial^2 T}{\partial x^2} = 0 \quad \text{for } 0 < x < d, \\ T(d, t) = T_R, \quad -\frac{\partial T}{\partial x}(0, t) = \frac{J_L}{\kappa}. \end{cases} \quad (40)$$

The finite difference approximation of the problem (40) based on above grid reads:

$$\begin{cases} T^0 - 3T^1 + 4T^2 = -\frac{J_L}{\kappa}, \\ \vdots \\ T^{k-1} - 2T^k + T^{k+1} = 0 \quad \text{for } k = 2, \dots, N-1, \\ \vdots \\ -T^{N-1} + 2T^N = T_R \end{cases} \quad (41)$$

Problem (40) has an analytical solution which is a linear function:

$$T(x) = -\frac{J_L}{\kappa}x + T_R \quad (42)$$

In Figure 4 calculated temperature distributions for selected times are presented. For calculations of problem (20) the following data were used: $\theta = 8.55 \cdot 10^{-5} m^2 \cdot s^{-1}$, ($\kappa = 202.4 W \cdot m^{-1} \cdot K^{-1}$), $J_L = 1000 W \cdot m^{-2}$, $T_R = 350 K$.

REFERENCES

- [1] Y. Jaluria, Fluid flow phenomena in materials processing – the 2000 freeman scholar lecture, J. Fluids Eng. **123**, 173-210 (2001).
- [2] R. Guthrie, Fluid flows in metallurgy – friend or foe? Metall. Mater. Trans. B **35**, 417-437 (2004).
- [3] M. Kieloch, Ł. Piechowicz, J. Boryca, A. Klos, Archives of Metallurgy and Materials **55** (3), 647-656 (2010).
- [4] A. Kulawik, A. Bokota, Archives of Metallurgy and Materials **56** (2), 345-357 (2011).
- [5] F. Durst, D. Melling, S. Oka, Development of fluid mechanics methods in the 20th century and the application to laminar and turbulent flow investigations, in Modeling Fluid Flow (eds J. Vad, T. Lajos, R. Schilling), Springer (2003), Berlin, 49-76.
- [6] P.A. Nikrityuk, Computational Thermo-Fluid Dynamics, in Materials Science and Engineering, Wiley-VCH, (2011), Chap. 2.

- [7] H.K. Versteeg, W. Malalasekera, An Introduction to Computational Fluid Dynamics. The finite Volume Method. (second edition), PEARSON – Prentice Hall, Glasgow, (2007).
- [8] W. Hackbusch, Multi-grid Methods and Applications, Springer (Series in Computational Mathematics), (2003).
- [9] B. Machulec, J. Buzek, Hutnik – Wiadomości Hutnicze, 12, 857-860 (2009).
- [10] <http://www.cyf-kr.edu.pl>
- [11] W.E. Schiesser, The Numerical Method of Lines, Academic Press, San Diego, 1991.

Received: 20 May 2012.